Japanese Journal of Applied Physics
Vol. 47, No. 9, 2008, pp. 7052–7055

©2008 The Japan Society of Applied Physics

Characterization of Intrinsic Defects in High-Purity High-Resistivity p-Type 6H-SiC

Hideharu MATSUURA*, Hirokazu YANASE, and Miyuki TAKAHASHI

Department of Electronic Engineering and Computer Science, Osaka Electro-Communication University, 18-8 Hatsu-cho, Neyagawa, Osaka 572-8530, Japan

(Received April 22, 2008; accepted June 14, 2008; published online September 12, 2008)

The densities, cross sections, and energy levels of intrinsic defects in high-purity high-resistivity (approximately $10^6\,\Omega\,\mathrm{cm}$) p-type 6H-SiC are determined using isothermal capacitance transient spectroscopy (ICTS). Five intrinsic defects are detected ranging from 0.76 to 1.35 eV above the valence band. Since the sum of the densities of intrinsic defects detected is the same order of magnitude as the acceptor density in the p-type 6H-SiC, the intrinsic defects are found to decrease the majority-carrier concentration making its resistivity as high as approximately $10^6\,\Omega\,\mathrm{cm}$. [DOI: 10.1143/JJAP.47.7052]

KEYWORDS: high-resistivity SiC, high-purity SiC, p-type SiC, 6H-SiC, deep level, hole trap, ICTS, intrinsic defect

1. Introduction

For the lateral-power microwave device applications of silicon carbide (SiC) and gallium nitride (GaN), a very high resistivity substrate with a low concentration of deep levels is required because deep levels in the substrate limit the maximum frequency and efficiency of the devices, and also degrade the stability. That is why the high-purity semi-insulating SiC substrate has been intensively investigated,[1–3] instead of the vanadium (V)-doped semi-insulating SiC. The resistivity (ρ) of high-purity SiC is strongly affected by intrinsic defects located in its midgap, which capture the majority carriers. Therefore, it is necessary to investigate the nature of the deep levels in high-purity SiC. Traps have been usually evaluated using deep-level transient spectroscopy (DLTS).[4,5] DLTS analysis is feasible only when trap densities are much lower than the dopant density.[6]

Because trap densities have the same order of magnitude as the density of unintentional impurities (donors or acceptors) in high-purity high-resistivity (HPHR) SiC, DLTS cannot be used to characterize its intrinsic defects. For this reason, to characterize the intrinsic defects in SiC, dopant-doped low-resistivity SiC irradiated by electrons has been intensively investigated by DLTS in the past.[7,8]

To investigate the intrinsic defects in HPHR SiC, isothermal capacitance transient spectroscopy (ICTS)[9] can be applied. However, DLTS and ICTS cannot be used for semi-insulating semiconductors with ρ much higher than $10^6\,\Omega\,\mathrm{cm}$ because the measured capacitance is determined by the thickness of the diode, and not by the depletion region of the junction.[10–15] In this paper, we report on our investigation on the intrinsic defects in HPHR p-type 6H-SiC from the temperature dependence of ICTS signals.

2. Experimental Procedure

The thickness and size of the HPHR 6H-SiC substrate grown by the modified Lely method were 1 mm and $5 \times 5\,\mathrm{mm}^2$, respectively. Ni electrode (so-called bottom electrode) was evaporated on one side of the sample, and then the sample was annealed to obtain good ohmic contact. After the cleaning of the other side of the sample, Ni electrode with a radius of 1 mm (so-called top electrode) was evaporated. The current–voltage (I–V) characteristics of the diode were measured using Keithley source-measure unit (SMU238). Capacitance–voltage (C–V) and transient capacitance $C(t)$ measurements were carried out at a frequency of 1 MHz in the temperature range between 300 and 600 K using Horiba Deep-Level Analyzer (DA-1500). The $C(t)$ was measured after an applied voltage was changed rapidly from 0 to a reverse bias (V_R) of -20 V.

3. Results

3.1 *I–V and C–V characteristics*

Figure 1 shows the I–V characteristics of the diode at 500 K. Here, the bias voltage in the figure was applied to the top electrode. The forward current flowed when the top electrode was negatively biased, whereas the reverse current flowed when it was positively biased, indicating that conduction in this highly resistive 6H-SiC is p type. From the slope of the I–V characteristics around the forward bias of 2 V, ρ of the 6H-SiC substrate was determined as approximately $10^6\,\Omega\,\mathrm{cm}$.

The capacitance of the diode at 300 K was independent of reverse bias, and was close to the geometric capacitance calculated using the thickness of the 6H-SiC substrate. At temperatures higher than 450 K, the capacitance was dependent on reverse bias, indicating that the measured capacitance is determined by the width of the depletion layer. Therefore, the capacitance was measured at temperatures higher than or equal to 450 K.

Figure 2 shows the C^{-2}–V characteristics of the diode at 500 K. From the slope, the value of N_A–N_D was estimated as $9.3 \times 10^{14}\,\mathrm{cm}^{-3}$, where N_A and N_D are the densities of the acceptors and donors, respectively.

3.2 *Isothermal capacitance transient spectroscopy*

Figure 3 shows the $C(t)$ and ICTS signal of the diode at 500 K, indicated by dashed and solid lines, respectively. Here, the ICTS signal $S(t)$ is defined as[9]

$$S(t) \equiv t\frac{\mathrm{d}C(t)^2}{\mathrm{d}t}. \tag{1}$$

From the number of peaks of $S(t)$ in Fig. 3, at least three types of hole-trap species could be detected. These hole traps are here referred to as HRH2, HRH3, and HRH4, as shown in Fig. 3. Judging from the ICTS signals in the shorter or longer time range, there are at least another two unresolved hole traps. However, Figs. 4 and 5 show the ICTS signal at 470 and 530 K, respectively, in which these two contribu-

*E-mail address: matsuura@isc.osakac.ac.jp

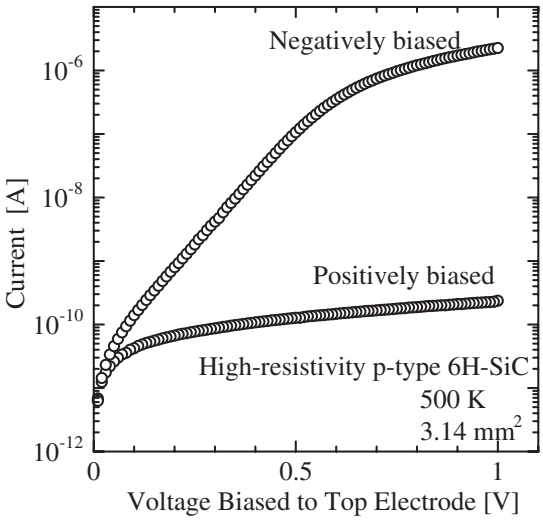

Fig. 1. *I–V* characteristics.

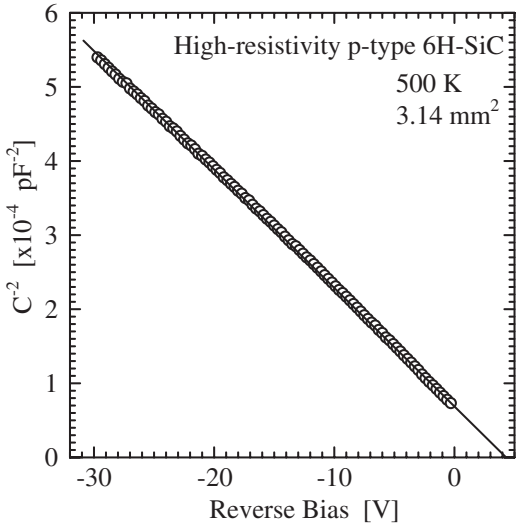

Fig. 2. $1/C^{-2}$–V characteristics.

tions could be fully resolved and labeled HRH1 and HRH5, respectively. Finally, five types of hole trap could be observed in the temperature range between 450 and 600 K.

The ICTS signal is theoretically expressed as[9)]

$$S(t) = \frac{q\epsilon_s\epsilon_0 A^2}{2(V_d - V_R)} \sum_i N_{ti} e_{ti} t \exp(-e_{ti} t), \tag{2}$$

which has a peak at

$$t_{peaki} = \frac{1}{e_{ti}}, \tag{3}$$

where A is the junction area, q is the electron charge, ϵ_s is the dielectric constant of semiconductor, ϵ_0 is the free-space permittivity, V_d is the diffusion potential of diode, N_{ti} and e_{ti} are the density and emission rate of the ith hole trap, respectively. Moreover, N_{ti} is given as[9)]

$$N_{ti} = \frac{2(V_d - V_R)}{q\epsilon_s\epsilon_0 A^2} S(t_{peaki}) \exp 1. \tag{4}$$

On the other hand, the hole concentration at the ith trap (p_{ti}) varies as[16–18)]

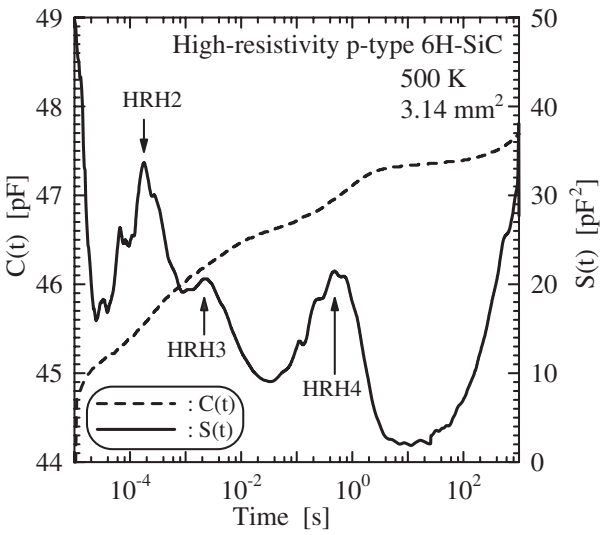

Fig. 3. Transient capacitance and ICTS signal at 500 K.

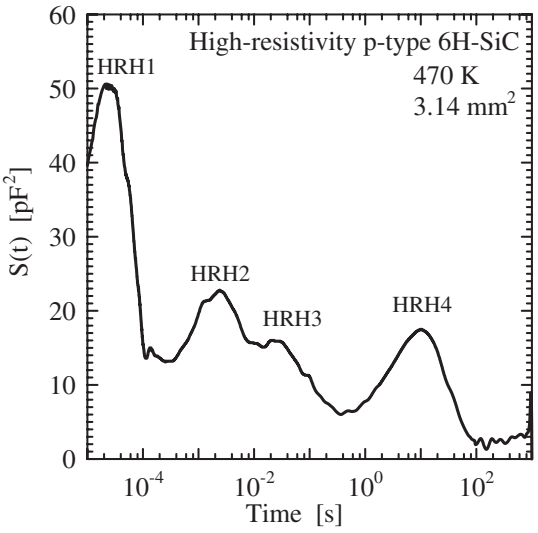

Fig. 4. ICTS signal at 470 K.

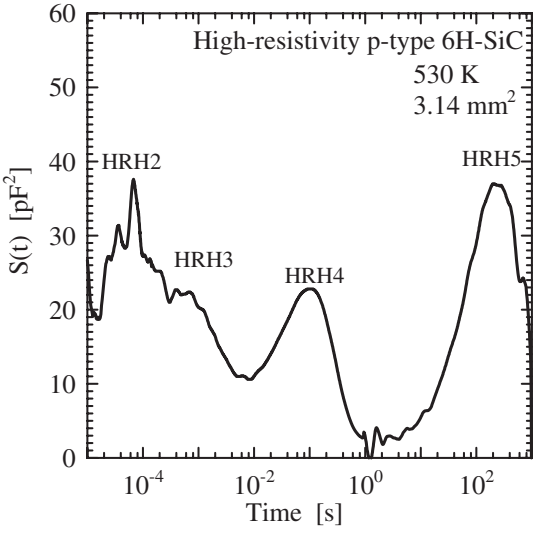

Fig. 5. ICTS signal at 530 K.

$$\frac{dp_{ti}}{dt} = \sigma_{ti} v_{th} p(N_{ti} - p_{ti}) - e_{ti} p_{ti}, \quad (5)$$

where

$$p_{ti} = N_{ti}[1 - f(E_{ti})], \quad (6)$$

$f(E_{ti})$ is the electron occupation probability for the ith hole trap, given as

$$f(E_{ti}) = \frac{1}{1 + g_{ti} \exp\left(\frac{E_{ti} - E_F}{kT}\right)}, \quad (7)$$

p is the hole concentration in the valence band, expressed as

$$p = N_V \exp\left(-\frac{E_F - E_V}{kT}\right), \quad (8)$$

v_{th} is the thermal velocity of electron, E_F is the Fermi level, N_V is the effective density of states in the valence band, E_V is the valence band maximum, k is the Boltzmann constant, T is the absolute temperature, and E_{ti}, σ_{ti}, and g_{ti} are the energy level, cross section, and degeneracy factor of the ith hole trap, respectively. In thermal equilibrium ($dp_{ti}/dt = 0$), e_{ti} is derived using eqs. (5)–(8) as

$$e_{ti} = \frac{N_V \sigma_{ti} v_{th}}{g_{ti}} \exp\left(-\frac{E_{ti} - E_V}{kT}\right). \quad (9)$$

Since N_V is proportional to $T^{1/2}$ and v_{th} is proportional to $T^{3/2}$, the emission rate is expressed as

$$e_{ti} = B_i \sigma_{ti} T^2 \exp\left(-\frac{E_{ti} - E_V}{kT}\right) \quad (10)$$

and

$$B_i = \frac{4\pi\sqrt{6\pi} m_h^* k^2}{g_{ti} h^3}, \quad (11)$$

where m_h^* is the hole effective mass and h is Planck's constant. On the basis of the discussion above, the relationship between e_{ti}/T^2 and $1/T$ is shown in Fig. 6. In Fig. 6, the optimum straight line fitting to experimental data for each trap could be obtained, from which the values of E_{ti} and σ_{ti} could be determined and listed in Table I. Here, m_h^* and

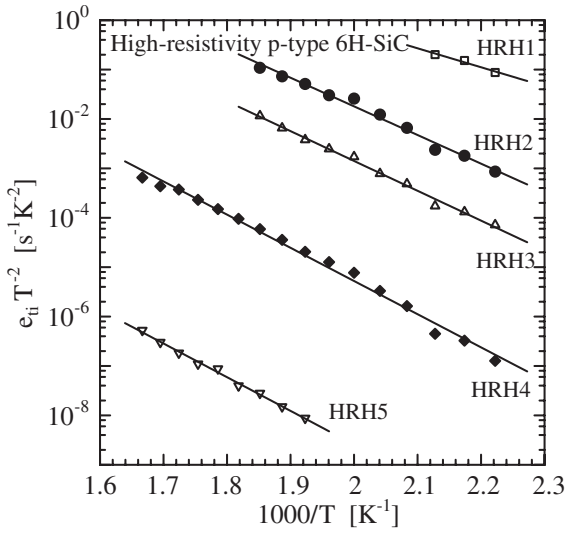

Fig. 6. Relationship between e_{ti}/T^2 and $1/T$.

Table I. Densities, energy levels and cross sections of hole traps determined from ICTS.

Hole-trap species	Density (cm^{-3})	Energy level (eV)	Cross section (cm^2)
HRH1	5.0×10^{13}	$E_V + 0.76$	1×10^{-14}
HRH2	3.3×10^{13}	$E_V + 1.15$	2×10^{-12}
HRH3	2.0×10^{13}	$E_V + 1.20$	5×10^{-13}
HRH4	2.1×10^{13}	$E_V + 1.33$	4×10^{-14}
HRH5	3.6×10^{13}	$E_V + 1.35$	4×10^{-17}

g_{ti} were assumed to be m_0 and 1, respectively, where m_0 is the electron rest mass. This table also includes N_{ti} estimated using eq. (4), which is averaged over the temperature range of the measurement.

4. Discussion

There are few reports on deep levels in p-type SiC in the literature, and also, it is difficult to characterize electrically active deep levels in high-resistivity or semi-insulating SiC. In 6H-SiC, deep levels denoted by H1 and H2 were reported to be located at $E_V + 0.55$ eV and $E_V + 0.78$ eV, respectively.[19] By photoexcitation-electron-paramagnetic-resonance studies, a deep level (EI5) relating to the positively charged carbon vacancy (V_C) was reported to exist in electron-irradiated p-type 4H-SiC lying at $E_V + 1.47$ eV.[20] According to DLTS studies on deep levels in low-resistivity p-type 4H-SiC epilayers,[7,8] the following deep levels were reported; D with an energy level of $E_V + 0.49$ eV and a cross section of 1×10^{-16} cm^2, HK0 with $E_V + 0.79$ eV and 3×10^{-16} cm^2, HK2 with $E_V + 0.84$ eV and 4×10^{-14} cm^2, HK3 with $E_V + 1.27$ eV and 3×10^{-14} cm^2, and HK4 with $E_V + 1.44$ eV and 6×10^{-15} cm^2. According to literature,[21] E_V in 6H-SiC is the same energy position as E_V in 4H-SiC, whereas the conduction-band minimum in 6H-SiC is lower than that in 4H-SiC. Since the energy levels of hole traps are measured from the E_V, the energy levels of the hole trap of the same origin in 6H-SiC and 4H-SiC are considered to be similar. On the basis of the dependence of the deep-level density on the fluence of electron irradiation,[8] the origin of HK4 was reported to be a complex including V_C, whereas HK0 might not be related to V_C. Compared with our results, the origins of HRH1, HRH3, and HRH4 in 6H-SiC might be considered to be those of HK2, HK3, and HK4 in 4H-SiC, respectively.

The sum of the densities of intrinsic defects detected is 1.6×10^{14} cm^{-3}, whereas the acceptor density is approximately 9×10^{14} cm^{-3}. Therefore, the intrinsic defects strongly decrease the majority-carrier concentration in the high-purity 6H-SiC, which makes ρ as high as approximately 10^6 Ω cm.

5. Conclusions

In high-resistivity semiconductors, the temperature range for the capacitance measurement was limited because the capacitance of a diode at low temperatures was determined by the thickness of the sample, and not by the width of the depletion region of the junction. Furthermore, the sum of the densities of the deep levels was close to the dopant density. Even in the case mentioned above, it was demonstrated that

ICTS could be used to determine the densities and energy levels of deep levels. In HPHR p-type 6H-SiC, five deep levels were detected by ICTS. By comparison of the sum of the densities of detected intrinsic defects with the acceptor density, these intrinsic defects were found to make ρ as high as approximately $10^6\,\Omega\,\mathrm{cm}$.

Acknowledgments

This work was partially supported by the Academic Frontier Promotion Projects of the Ministry of Education, Culture, Sports, Science and Technology in 1998–2002 and 2003–2008, and partially supported by a Grant-in-Aid for Scientific Research (C) from the Japan Society for the Promotion of Science in 2006 and 2007 (18560356).

1) U. Gerstmann, E. Rauls, and H. Overhof: Phys. Rev. B **70** (2004) 201204.
2) R. Aavikko, K. Saarinen, F. Tuomisto, B. Magnusson, N. T. Son, and E. Janzén: Phys. Rev. B **75** (2007) 085208.
3) W. C. Mitchel, W. D. Michell, H. E. Smith, G. Landis, S. R. Smith, and E. R. Glaser: J. Appl. Phys. **101** (2007) 053716.
4) D. V. Lang: J. Appl. Phys. **45** (1974) 3023.
5) D. K. Schroder: *Semiconductor Materials and Device Characterization* (Wiley, New York, 1998) 2nd ed., pp. 276 and 290.
6) H. Matsuura, H. Iwata, S. Kagamihara, R. Ishihara, M. Komeda, H. Imai, M. Kikuta, Y. Inoue, T. Hisamatsu, S. Kawakita, T. Ohshima, and H. Itoh: Jpn. J. Appl. Phys. **45** (2006) 2648.
7) K. Danno and T. Kimoto: Jpn. J. Appl. Phys. **45** (2006) L285.
8) K. Danno and T. Kimoto: Mater. Sci. Forum **556–557** (2007) 331.
9) H. Okushi and Y. Tokumaru: Jpn. J. Appl. Phys. **19** (1980) L335.
10) H. Matsuura, T. Okuno, H. Okushi, and K. Tanaka: J. Appl. Phys. **55** (1984) 1012.
11) H. Matsuura: J. Appl. Phys. **64** (1988) 1964.
12) H. Matsuura: J. Appl. Phys. **68** (1990) 1138.
13) H. Matsuura and H. Okushi: in *Amorphous and Micro-Crystalline Semiconductor Devices Vol. II: Materials and Device Physics*, ed. J. Kanicki (Artech House, Boston, MA, 1992) Chap. 11.
14) H. Matsuura, M. Takahashi, S. Nagata, and K. Taniguchi: J. Mater. Sci.: Mater. Electron. **19** (2008) 810.
15) M. Takahashi and H. Matsuura: *Proc. Int. Conf. Silicon and Carbide and Related Materials 2007, Otsu, 2007*, to be published in Mater. Sci. Forum.
16) A. G. Milnes: *Deep Impurities in Semiconductors* (Wiley, New York, 1973) p. 116.
17) J. Singh: *Semiconductor Devices: An Introduction* (McGraw-Hill, New York, 1994) p. 172.
18) K. F. Brennan: *The Physics of Semiconductors with Applications to Optoelectronic Devices* (Cambridge University Press, Cambridge, U.K., 1999) p. 499.
19) A. Kawasuso, M. Weidner, F. Redmann, T. Frank, P. Sperr, G. Kögel, M. Yoshikawa, H. Itoh, R. Krause-Rehberg, W. Triftshäuser, and G. Pensl: in *Silicon Carbide*, ed. W. J. Choyke, H. Matsunami, and G. Pensl (Springer, Berlin, 2004) p. 577.
20) N. T. Son, B. Magnusson, and E. Janzén: Appl. Phys. Lett. **81** (2002) 3945.
21) V. V. Afanas'ev, M. Bassier, G. Pensl, M. J. Schulz, and E. Stein von Kamienski: J. Appl. Phys. **79** (1996) 3108.